31st Annual International Conference of the IEEE EMBS
Minneapolis, Minnesota, USA, September 2-6, 2009

Validation of a Novel Three-Dimensional Electrode Array within Auditory Cortex

Nicholas B. Langhals, *Member, IEEE* and Daryl R. Kipke, *Member, IEEE*

***Abstract*—Three-dimensional electrode arrays have a variety of potential applications in the fields of both intracortical mapping as well as basic research studies designed to characterize and understand the physiology of the brain. While higher channels counts are desired in brain-machine interface applications, the ability to analyze synchronous data from multiple cortical locations, including various depths is pivotal to fully mapping the underlying neurophysiology of sensory cortices. Within this study, we present a proof of concept validation of a 3D probe technology consisting of 16 silicon shanks in a 4x4 grid arrangement with four electrode sites per shank. This 3D array has been implanted in a rat primary auditory cortex and electrophysiological data are presented showing the utility of electrode sites spanning multi-lateral cortical space as well as cortical depth.**

I. Introduction

Neural probe technology has many different clinical and research applications including disease characterization and understanding underlying neurophysiology. The structural characteristics of the brain, as studied anatomically or through imaging, yield valuable information about the expected function of the underlying neural system [1]. However, imaging and anatomical characterization lack the resolution and desired output metrics that are paramount to understanding how the firing of individual neurons and ensembles combine to create sensory perception or even consciousness.

To better understand and interpret the neural firing patterns within the brain, new technological advances are required that incorporate the use of high channel counts that can simultaneously sample from large populations of neurons to yield more information about the underlying cortical morphology and structure. Many neural probe technologies currently exist that incorporate high numbers of electrode sites assembled from a large number of individual microwires [2, 3]. While these technologies achieve the throughput of information necessary for controlling external devices and brain-computer interfaces, they lack the ability to sample from a three-dimensional volume of neural tissue simultaneously [4]. Other microfabricated structures can sample high channel counts and have been used in cortical mapping experiments, but these devices are only capable of sampling from a planar representation of the cortex [5-9]. The simultaneous sampling of neural tissue in 3D creates the possibility of mapping neural connections within the brain and understanding how these networks create sensory perceptions from firing of individual neurons.

In order to move towards 3D electrode sampling, we have tested a new 64-channel electrode array implanted into the auditory cortex of a rat. The functionality of the electrode array was validated in three different capacities within this study to verify device utility and functionality following insertion. First, gross recording quality was examined immediately following insertion to verify that the minimal trauma is consistent with similar probe technologies. Second, auditory-driven activity was used to verify that the device was implanted into an auditory cortical region of the brain and localized neural circuits remained intact. Finally, frequency response maps of the primary auditory cortex were constructed to verify a typical and unaltered tonotopic architecture.

II. Methods

A. Electrode Array

The electrode arrays used in this study consisted of prototype 3D probes assembled by NeuroNexus Technologies (Ann Arbor, MI). These were created by horizontally stacking four commercially available acute devices using a polymer interconnect to separate the individual probes for uniform spacing. Sixteen electrode

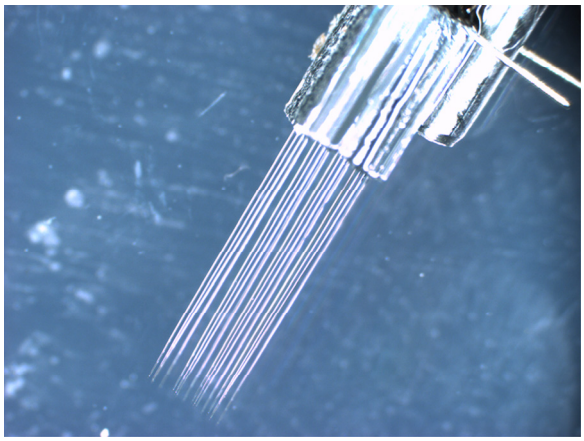

Figure 1. Image of example 3D probe style as used in this study. The 16 shanks are spaced at 200 µm and each set of shanks is spaced at about 200 µm between them.

Manuscript received April 23, 2009. This work was supported in part by the Center for Neural Communication Technology - a P41 Resource Center funded by the National Institute of Biomedical Imaging and Bioengineering (NIBIB, P41 EB002030) and supported by the National Institutes of Health (NIH).s This research was also partially funded through a grant by the University of Michigan Coulter Translational Research Partnership Award.

N. B. Langhals and D. R. Kipke are with the University of Michigan Department of Biomedical Engineering, Ann Arbor, MI 48109 USA (734-615-9401; fax: 734-647-4834; e-mail: langhals@umich.edu).

shanks of four sites each were arranged in a 4x4x4 grid for a total of 64 electrode sites. The individual shanks were three mm in length with 177 µm^2 sites spaced at 50 µm apart (Fig. 1).

B. Surgery

All implants in this study were performed on male Sprague-Dawley rats targeting primary auditory cortex. Surgical procedures were similar to those used previously [7, 10]. Initial anesthesia was administered via intraperitoneal injection of a mixture of 50 mg/mL ketamine, 5 mg/mL xylazine, and 1 mg/mL acepromazine at an injection volume of 0.125 mL/100 g body weight. Updates were given throughout the procedure at a dosage of 0.1 mL ketamine (50 mg/mL) as needed to maintain a consistent depth of anesthesia. Animals were secured in a standard stereotaxic frame (myNeurolab, St. Louis, MO). A 316 SS stainless steel bonescrew was inserted anterior to bregma so that it barely touched the surface of the brain and was used as a reference and ground for all recordings in the experiment.

After removing excess muscle and tissue on the side of the head, a craniotomy approximately 4 x 4 mm was made over primary auditory cortex. The dura was resected in order to allow for probe insertion and the exact target was located using the well-defined vascular landmarks that have been reported previously [11]. The 3D electrode array was then mounted to the stereotaxic manipulator and driven perpendicular to the cortical surface in to a target depth of 1 mm so that the deepest electrode sites were located near layer IV. All procedures complied with the U.S. Department of Agriculture guidelines for the care and use of laboratory animals and were approved by the University of Michigan Animal Care and Use Committee.

C. Electrophysiology

All recordings were acquired using a TDT multi-channel acquisition system (RZ2, Tucker-Davis Technologies, Alachua, FL) in an electrically and acoustically shielded

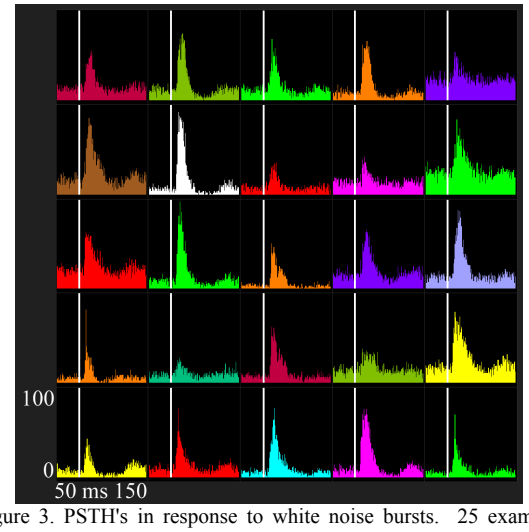

Figure 3. PSTH's in response to white noise bursts. 25 example good channels. Tone onset is represented by the solid white line. Data for each channel ranges from 50 ms prior to tone onset up to 150 ms after.

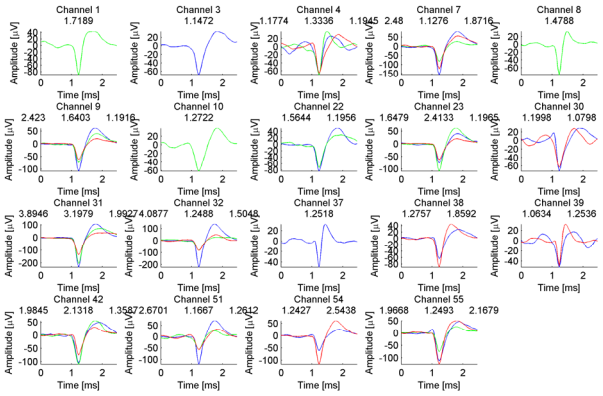

Figure 2. Example mean spike waveforms of units recorded from the 3D array. Different colored waveforms show that a large number of channels have multiple unit waveforms present. The numbers above the plots indicate the signal-to-noise ratio of the presented mean waveform.

booth. Neural electrophysiological recordings for all 64 channels were fed through an anti-aliasing filter (0.35 Hz – 7.5 kHz) amplified, and sampled at ~50 kHz. During real-time processing, the signals were separated into spike (300 - 5000 Hz) and local field potential (2 - 300 Hz) bands through further filtering, otherwise wideband data for post-processing unit characterization was filtered from 2 - 5000 Hz.

During all recording sessions, either white-noise bursts or individual tones generated by the TDT RZ2 were played through a free-field speaker in the sound-isolation booth. White noise bursts were created by taking flat spectrum random noise and low-pass filtering the signal at 10 kHz. These bursts were presented for 10 ms at four times per second to the subject. Each single frequency tone was presented for 125 ms at four presentations per second. Each tone was cosine gated on and off with a rise/fall time of 5-ms to avoid transient speaker clicks from step amplitude changes [12]. Tone amplitudes ranged from 0.1 - 4V and frequencies ranged from 500 Hz - 16 kHz. Tones were repeated 50 times to allow for signal averaging in the histograms.

D. Data Filtering and Analysis

Wideband neural recording segments were analyzed off-line using custom automated MATLAB (Mathworks, Natick, MA) software, as described in detail elsewhere [7]. Briefly, an amplitude discrimination threshold was set at 3.5 standard deviations above and below the mean of the recording segments. For each peak exceeding the threshold, a 2.4-ms candidate waveform snippet centered on the absolute minimum of the waveform was removed from the recorded segment and stored. The peak-to-peak noise level was calculated as six times the standard deviation of the remaining data. After initial principal component analysis, individual clusters were identified using fuzzy c-means clustering. After clustering, waveforms with a cluster membership index of greater than 0.8 were used to determine a mean waveform for a cluster. The signal-to-

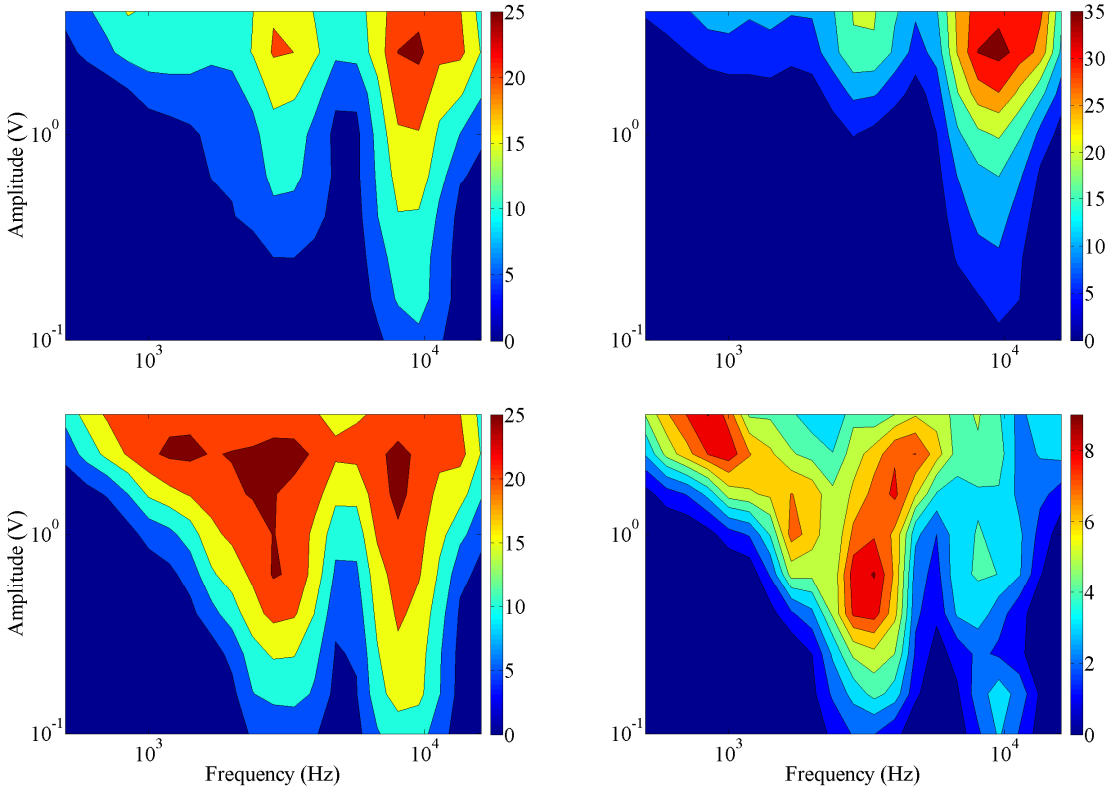

Figure 4. Frequency response maps of 4 electrode sites on different shanks of the array. The x-axis is the frequency of the presented tone, the y-axis is the amplitude in volts and color axis is indicative of the z-score for the individual frequency / amplitude combination. All data has been smoothed by convolving with a normalized 5x5 Gaussian window after insignificant responses of $p<0.01$ have been removed. Each row of electrode sites falls on about the same tonotopic line, with upper row having a best frequency of 9.5 kHz, while the lower row has a best frequency of 3.3 kHz.

noise ratio for these waveforms was calculated as the peak-to-peak amplitude of the waveform divided by the calculated noise value. Values of greater than 1.1 are considered quality units that are easily discriminable from the underlying noise floor.

For all other data, a real-time amplitude threshold was set to discriminate candidate waveforms from the noise. For each crossing, a candidate waveform was acquired using the integrated thresholding within the TDT software. Each of these 2.4 ms snippet waveforms was saved and used for all other processing. All spikes recorded as snippets were assumed to be multi-unit clusters or combinations of multiple units for all further analysis. Local field potential activity was down-sampled to 3 kHz and also saved for offline analysis.

E. Frequency Response Analysis

The frequency response maps were created by first taking all spike events and creating histograms of the spike times surrounding the event for the tone presentation. The spikes were accumulated into bins of 1-ms in duration for periods of time around the tone presentation. The 50 ms prior to tone presentation was used as baseline data and the 50 ms following tone onset was used to create the response window. The mean value of the response window was then compared to the cumulative mean and standard deviation of the channel in the pre-stimulus period to calculate a z-score indicating significance of response. Insignificant z-scores of less than 2.33, corresponding to a $p<0.01$, were set to zero and the response map was smoothed using a 5-point 2D Gaussian convolution.

III. Results and Discussion

High quality neural spike waveforms were recorded in all sessions using the wide-band recording data. Neural spikes were recorded immediately following device insertion, suggesting that increased damage had not occurred during device insertion relative to comparable insertions of 3D arrays. Mean waveforms output from the clustering algorithm are shown in Fig. 2. Signal-to-noise ratios shown ranged from 1.1 to 3.9 indicating that signal quality was also comparable with typical unit activity recorded from 2D arrays.

Individual channel activity was analyzed to examine the auditory-driven response characteristics of the implanted electrode arrays. White noise bursts trigger a delayed onset increase in neural firing rates of electrodes implanted in primary auditory cortex. Peri-stimulus time histograms of spike counts around the onset of the presented white noise burst are shown in Fig. 3. Twenty-five channels showed significantly large driven activity with an onset response that occurred 8-12 ms following the start of the presentation of the white noise, which is the expected delay arising from the number of synapses to the primary auditory cortex.

We created frequency response maps to measure the

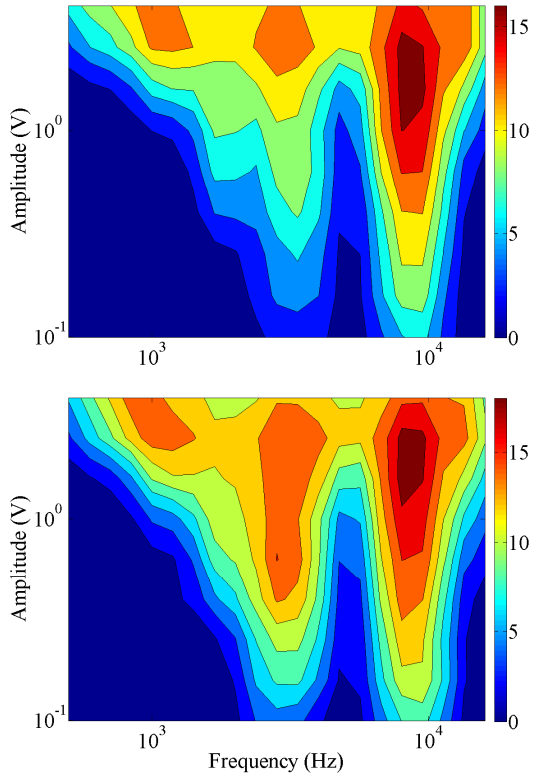

Figure 5. Frequency response maps of 2 adjacent electrode sites on the same shank of the array. The x-axis is the frequency of the presented tone, the y-axis is the amplitude in volts and color axis is indicative of the z-score for the individual frequency / amplitude combination. All data has been smoothed with a normalized 5x5 Gaussian window.

tonotopic organization of the recorded units to evaluate the consistency of the tonotopic structure following device insertion. Fig. 4 shows four example response maps covering electrode sites from four edges of the implanted 3D array. The best frequency for each of these maps was defined as the frequency that elicited a significant response of $p<0.01$ at the lowest available presented amplitude. The best frequencies for these four electrodes ranged from 3 kHz to 10 kHz.

Two electrode sites on the same shank spaced at 200 microns are depicted in Fig. 5. These maps have approximately the same bimodal shape with multiple best frequencies centered around 3 kHz and 9 kHz. This consistent structure is expected based on the tonotopic organization of the cortex and the placement of the 3D array such that a given row of shanks falls on a tonotopic line of consistent frequency and an individual shank should have a similar response as a function of depth. All tonotopic maps suggest that 3D device insertion does not create substantially more damage from insertion than maps typically observed with the insertion of 2D arrays into the auditory cortex.

In this study, we have provided proof of concept validation of a novel 3D architecture neural probe. The array was successfully inserted into the rat cortex with neural recordings obtained soon following insertion, which suggests that the insertion trauma is comparable to conventional single or multi-shank microelectrode arrays. We recorded auditory-driven activity indicating that the neural circuits in the cortex remained intact. Finally, we measured frequency response maps showing that the tonotopic organization of auditory cortex is expected architecture. These results combine to provide a solid, proof of concept validation of this 3D probe architecture. This work promotes future studies directed at utilizing this technology to its fullest potential for exploring interconnectivity of neurons within the brain and mapping the neurophysiology of neural systems.

IV. Acknowledgment

The authors would like to thank Dr. Rio Vetter for surgical assistance, Dr. Kip Ludwig, Rachel M. Miriani, Takashi D. Y. Kozai, and Paras Patel for helpful discussions and paper review, and the rest of the Neural Engineering Lab at the University of Michigan. N.B Langhals is a consultant for NeuroNexus Technologies. D.R. Kipke has a significant financial interest in NeuroNexus Technologies.

V. References

[1] R. Kotter and E. Wanke, "Mapping brains without coordinates," *Philos Trans R Soc Lond B Biol Sci*, vol. 360, (no. 1456), pp. 751-66, Apr 29 2005.

[2] I. Ulbert, E. Halgren, G. Heit, and G. Karmos, "Multiple microelectrode-recording system for human intracortical applications," *J Neurosci Methods*, vol. 106, (no. 1), pp. 69-79, Mar 30 2001.

[3] A.B. Schwartz, "Cortical neural prosthetics," *Annu Rev Neurosci*, vol. 27, pp. 487-507, 2004.

[4] M.A. Lebedev and M.A. Nicolelis, "Brain-machine interfaces: past, present and future," *Trends Neurosci*, vol. 29, (no. 9), pp. 536-46, Sep 2006.

[5] A.A. Aarts, H.P. Neves, I. Ulbert, L. Wittner, L. Grand, M.A. Fontes, S. Herwik, S. Kisban, O. Paul, P. Ruther, R.P. Puers, and C. Van Hoof, "A 3D slim-base probe array for in vivo recorded neuron activity," *Conf Proc IEEE Eng Med Biol Soc*, vol. 2008, pp. 5798-801, 2008.

[6] T.J. Blanche, M.A. Spacek, J.F. Hetke, and N.V. Swindale, "Polytrodes: high-density silicon electrode arrays for large-scale multiunit recording," *J Neurophysiol*, vol. 93, (no. 5), pp. 2987-3000, May 2005.

[7] K.A. Ludwig, R.M. Miriani, N.B. Langhals, M.D. Joseph, D.J. Anderson, and D.R. Kipke, "Using a common average reference to improve cortical neuron recordings from microelectrode arrays," *J Neurophysiol*, vol. 101, (no. 3), pp. 1679-89, Mar 2009.

[8] J. Csicsvari, D.A. Henze, B. Jamieson, K.D. Harris, A. Sirota, P. Bartho, K.D. Wise, and G. Buzsaki, "Massively parallel recording of unit and local field potentials with silicon-based electrodes," *J Neurophysiol*, vol. 90, (no. 2), pp. 1314-23, Aug 2003.

[9] J. Du, I.H. Riedel-Kruse, J.C. Nawroth, M.L. Roukes, G. Laurent, and S.C. Masmanidis, "High-resolution three-dimensional extracellular recording of neuronal activity with microfabricated electrode arrays," *J Neurophysiol*, vol. 101, (no. 3), pp. 1671-8, Mar 2009.

[10] R.J. Vetter, J.C. Williams, J.F. Hetke, E.A. Nunamaker, and D.R. Kipke, "Chronic neural recording using silicon-substrate microelectrode arrays implanted in cerebral cortex," *IEEE Trans Biomed Eng*, vol. 51, (no. 6), pp. 896-904, Jun 2004.

[11] S.L. Sally and J.B. Kelly, "Organization of auditory cortex in the albino rat: sound frequency," *J Neurophysiol*, vol. 59, (no. 5), pp. 1627-38, May 1988.

[12] J.G. Arenberg, S. Furukawa, and J.C. Middlebrooks, "Auditory cortical images of tones and noise bands," *J Assoc Res Otolaryngol*, vol. 1, (no. 2), pp. 183-94, Sep 2000.